

Supplementary Material for the Curve Breaking Velocity Estimator (CBVE)

Kamran Ghaffari Toiserkan, József Kövecses, and Paul Karam

I. NOTES

This documents intends to provide more supporting material for the CBVE [1]. A sample code for the algorithm is also suggested at the end of the document.

II. SIMULATION RESULTS

In this section the performance of the CBVE algorithm in frequency and time domains is evaluated and compared to a few popular velocity estimation methods. The frequency response reveals important information about the performance of a LTI system. For a non-linear time-variant system, however, the frequency response is dependent upon the amplitude and bias (zero-offset) of the input signal. Considering the non-linearity introduced by quantization, we employed two different position signals of: a) $x(t) = 30q \sin(2\pi ft)$; and b) $x(t) = 3q \sin(2\pi ft)$, to study the frequency response of the estimation process. The two selected input signals represent the low and high amplitude regimes of encoder behavior, where, q is the encoder quantum, and f is the frequency of oscillation. The test was performed at 2 kHz sampling rate employing the following techniques: CBVE, best-fit FOAW [2], Linear Tracking Differentiator (LTD) [3], AFD [4], and a Band-Pass Filter (BPF) with $\omega_c = 150$ rad/s. The produced results are presented in Fig. 1. These results are identical for different encoder resolutions. To have more meaningful Bode plots, the measured magnitudes and phase lags in Fig. 1 are demonstrated with respect to the actual velocity not the incoming position signal. The dashed segments in the plots correspond to the frequencies at which the estimator could not perform a legitimate estimation. The spiky segments represent the sensitivity of the performance of estimators to the synchronization between encoder pulses and sampling instants which varies at different signal frequencies. A change in signal frequency affects the rate of change of the encoder pulses which results in different quality of samples at a fixed sampling rate.

Figure 1.a depicts that at higher amplitude oscillations, the CBVE has the smallest phase lag and attenuation property among the employed techniques while offering a relatively persistent performance. As can be seen, the phase lag of the CBVE estimates slightly increases at higher oscillation frequencies which can be reduced by increasing the sampling rate. In the case of lower amplitude oscillations (shown in

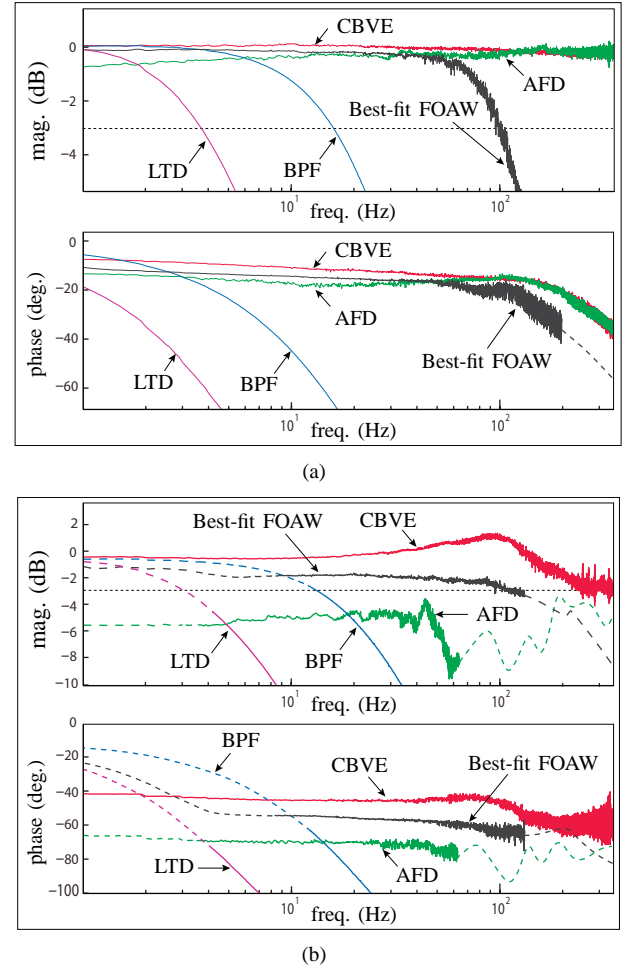


Fig. 1: Frequency response of different velocity estimators when excited with a sinusoidal position signal with peak amplitude of: (a) thirty, and (b) three, encoder resolutions.

Fig. 1.b.), the performance of the estimators is significantly reduced as the result of fewer encoder pulses per one oscillation cycle. In fact, the CBVE is the only method which maintained its functionality all over the excitation frequency window (from 1 to 350 Hz). All the other techniques were dominated by noise at low frequencies, and they were inefficient at high frequencies. This advantage becomes more important considering that every converging oscillating system will pass through low amplitude oscillation zone before coming to a complete stop. If a filter fails to operate efficiently at low amplitude oscillations, it will have a negative effect on the stability. To avoid this, the CBVE automatically disconnects its feedback before becoming inefficient at very low oscillation amplitudes.

K. Ghaffari T. and J. Kövecses are with the Department of Mechanical Engineering and Centre for Intelligent Machines, McGill University, Montreal, Québec, Canada, (kamran@cim.mcgill.ca; jozsef.kovecses@mcgill.ca)

P. Karam is with Quanser Inc., 119 Spy Court, Markham, Ontario, L3R 5H6, Canada (paul.karam@quanser.com)

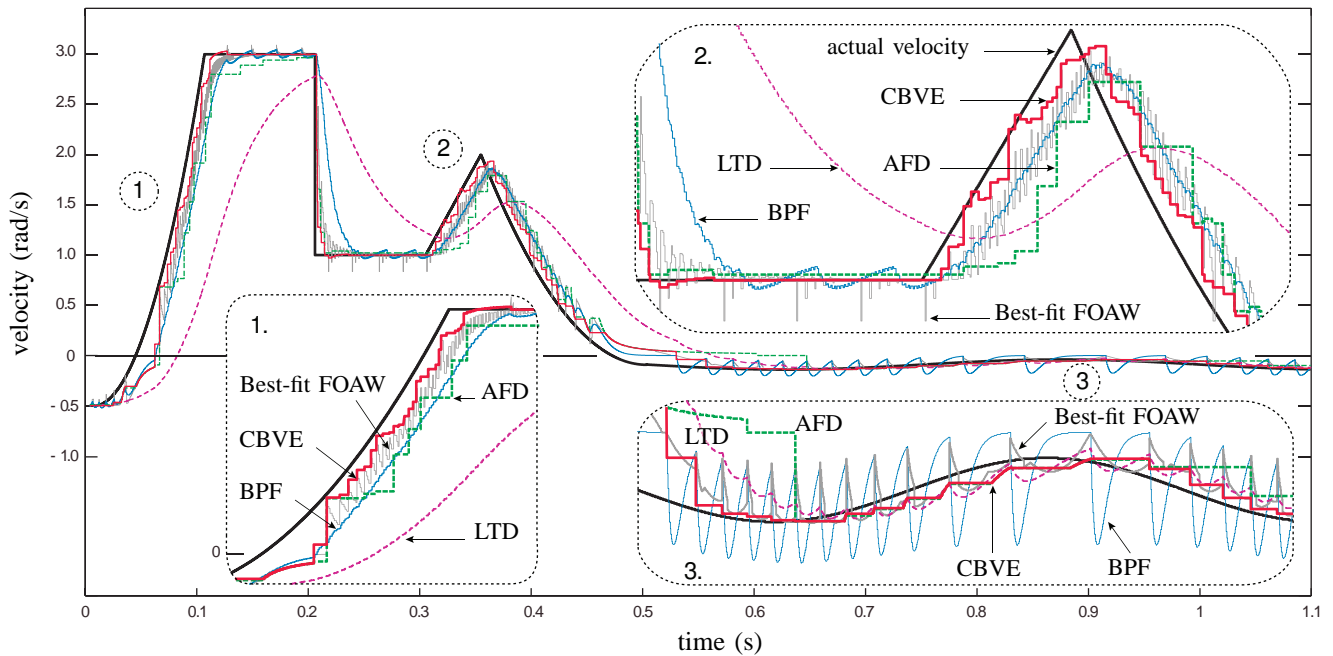


Fig. 2: A comparison between estimations of different velocity estimators to an arbitrary velocity profile.

Next, we study the performance of the estimators in time-domain. To this aim, we generated a velocity profile which incorporates different scenarios of constant, time-varying, sudden changing, zero crossing, and low velocities and sent its corresponding position signal to the estimators. The obtained velocity profiles are demonstrated in Fig. 2. As can be seen, the CBVE estimated profile has less time-delay than that of the other techniques. Moreover, the CBVE estimates are generally free of spikes and more accurate (especially at constant velocities). At low velocities, the estimates of the BPF, the FOAW, and the LTD are dominated by noise while the CBVE still provides reliable and spike-free estimations.

III. EXPERIMENTAL RESULTS

This section aims to demonstrate the ability of the CBVE to increase the efficiency of virtual dampers experimentally. In addition to the examples provided in [1], we employed a 6-DoF HD² Quanser haptic device [5] to render a three-dimensional rigid virtual box in space (see Fig. 3). In this experiment, the manipulator handle was considered to be trapped inside the virtual box with 10,000 N/m stiffness and 45 Ns/m damping for every side wall. To have the device interact with the virtual environment, the handle bar was released in a vertical orientation to hit the lower end of the box at $z = 10$ cm under its own weight. At the releasing instant the lower end-point of the handle bar was 10 cm above the lower side of the box, while the upper point of the handle was in contact with the upper side of the box. This robot is equipped with six high resolution optical encoders (with 4096 ppr accuracy) at its joints. The implemented controller could switch between the CBVE and a band-pass filter (BPF) with 150 rad/s cut-off frequency to estimate the joint velocities. The forward kinematics relation and the Jacobian matrix were used to obtain the workspace positions and velocities of each

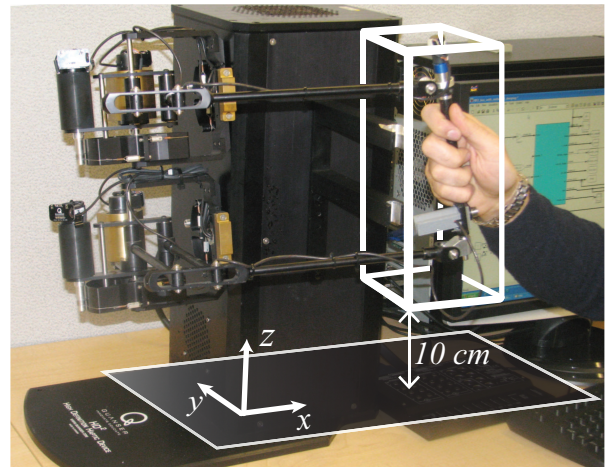
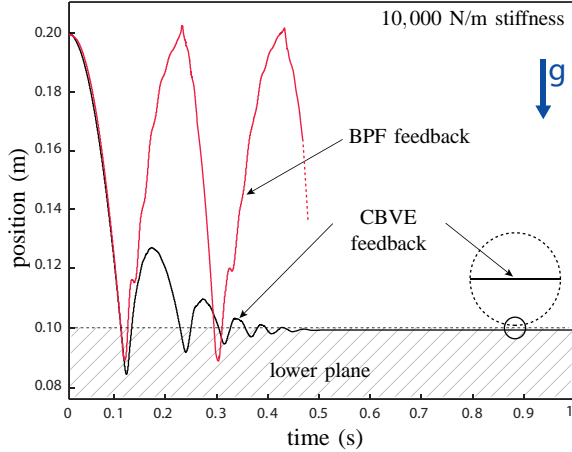


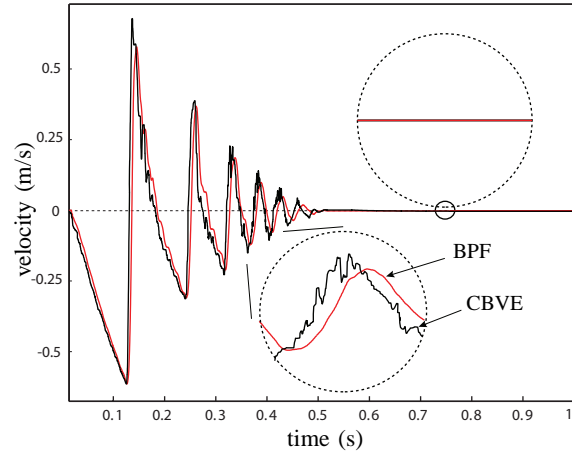
Fig. 3: The 6-DoF HD² Quanser haptic device.

end-point location of the handle bar. The appropriate control forces/torques could then be calculated to keep the released handle bar inside the virtual box (see the accompanying video of [1]). Fig. 4.a demonstrates the trajectory of the lower point of the handle bar in the z direction for both cases of the CBVE and the BPF estimation feedback. As can be seen, the controller with the CBVE feedback could successfully stabilize the motion, while the BPF feedback resulted the handle bar to bounce between the upper and lower planes of the box. The distortions in the trajectory for the active case is due to the coupled dynamics of the device and also the instantaneous contacts of the handle with the side walls during the motion. Fig. 4.b compares the velocity estimations of the CBVE with those of the BPF. As can be seen, the BPF velocity profile has a larger phase lag than that of the CBVE which also increases with the frequency of oscillation.

Moreover, the CBVE could display the transient distortions in



(a) Demonstration of the experimental trajectory in the z direction for the lower end of the handle bar.



(b) A comparison of the velocity profiles estimated by the CBVE and the band-pass filter.

Fig. 4

the velocity while the BPF could not distinguish the actual velocity changes from noise and resulted in estimating a smooth velocity profile. The distortions in the velocity are mainly caused by the coupled dynamics of the device and the temporal saturation of some of the actuators.

IV. CBVE SAMPLE CODE

The CBVE algorithm in MATLAB code:

```
% "TS" is the time stamping register
% "TS0" is the previous TS register
% "Xc" is the current measurement
% "Xp" is the previous measurement
% "cl" is the current time
% "t" is the instantaneous sampling time
% "Te" is the max expected timing error
% "BP" is the current breaking point
% "BP0" is the previous breaking point
% "q" is the quantization step
% "VF" is the current CBVE velocity
% "VF0" is the previous CBVE velocity
```

```
TS=zeros(3,60);
```

```
if (Xc~=Xp) % if there is a new event
    TS(:,(2:60))=TS0(:,(1:59));
    TS(1,1)=Xc; TS(2,1)=cl; TS(3,1)=t;
    BP=min(60,BP0+1); % initial breaking point
    Vu=10^(10); % initial velocity upper bound
    Vl=-10^(10); % initial velocity lower bound
    for i=2:BP
        for j=1:i-1
            T=TS(2,j)-TS(2,i); % time between the two events
            d=TS(1,j)-TS(1,i); % distance between the points
            Tmin=T-TS(3,i)-Te; % min time between the events
            Tmax=T+TS(3,j)+Te; % max time between the events
            V=d/T; % backward estimation

            euq=q/T; % quantization upper error bound
            elq=-q/T; % quantization lower error bound
```

```
% discretization error bounds
if Tmin>0
    eud=max(d*TS(3,i)/(T*Tmin),-d*TS(3,j)/(T*Tmax));
    eld=min(d*TS(3,i)/(T*Tmin),-d*TS(3,j)/(T*Tmax));
else
    eud=max(euq,-d*TS(3,j)/(T*Tmax));
    eld=min(elq,-d*TS(3,j)/(T*Tmax));
end

% common error bounds
euc=min(euq,eud);
elc=max(elq,eld);

% if the error ranges disjoin, break the loop!
if (V+euc)<Vl || (V+elc)>Vu BP=i-1; break;
end

% computing new intersection of all error ranges
if (V+euc)<Vu Vu=V+euc;
end
if (V+elc)>Vl Vl=V+elc;
end
end
if BP~=min(60,BP0+1) break;
end
end
VF=(Vu+Vl)/2;
VF=0.2*VF+0.8*VF0;% smoothed CBVE
RE=(Vu-Vl)/2; % max round-off error
% for upto 6 measurements per oscillation period VF=0
c=0; % dummy variable
for i=1:6
    S=sign(TS(1,i)-TS(1,i+1)+me);
    if S~=sign(TS(1,i+1)-TS(1,i+2)+me) c=c+1;
    end
    if c==2 VF=0;
    end
end
else % if this is not a new event
    TS=TS0;
    BP=BP0;
    T=cl-TS(2,1); % elapsed time since the last event
    euq=q/T;
    elq=-q/T;
    % "VF0" is the last estimated velocity
    if VF0>euq VF=euq;
    else if VF0<elq VF=elq;
        else VF=VF0;
        end
    end
end
end
```

ACKNOWLEDGMENT

The authors of this paper would like to thank and acknowledge the useful contributions and comments of Mr. Amin Abdossalami, and Mr. Amirpasha Javid in the implementation of the algorithm on the HD² device at Quanser Inc. The research work reported here was supported by the Natural Sciences and Engineering Research Council of Canada, Quanser Inc., and the Canadian Space Agency. The financial support is gratefully acknowledged.

REFERENCES

- [1] K. Ghaffari T., J. Kövecses, and P. Karam, "Haptic Rendering of Stiff Virtual Environments: The Curve Breaking Velocity Estimator," *Submitted for review to the IEEE Trans. on Robotics*, Sep. 2011.
- [2] F. Janabi-Sharifi, V. Hayward, and C.-S.J. Chen, "Discrete-time Adaptive Windowing for Velocity Estimation," *IEEE Trans. Cont. Sys. Tech.*, **8**, 1003-1009, Nov. 2000.
- [3] Y.X. Su, C.H. Zheng, and P.C. Muller, "A Simple Linear Velocity Estimator for High-Precision Motion Control," *IEEE Int. Conf. Emerging Tech. Factory Autom.*, 23-29, Sep. 2006.
- [4] K. Ghaffari T., J. Kövecses, and P. Karam, "Adaptive Frequency Differentiation: an Approach to Increase the Transparency and Performance of Haptic Devices," *IEEE Int. Conf. Rob. Autom.*, May 2011, China.
- [5] www.quanser.com